JTTEE5 17:574–582
DOI: 10.1007/s11666-008-9210-4
1059-9630/$19.00 © ASM International

Peer Reviewed

Effect of Cathode Microstructure on Arc Velocity and Erosion Rate of Cold-Sprayed Copper Cathodes in a Magnetically Rotated Atmospheric Pressure Arc

Keith D'Sa, Lakshminarayana Rao, and Richard J. Munz

(Submitted January 10, 2008; in revised form June 20, 2008)

Atmospheric pressure arc velocity and erosion measurements were performed on cold-sprayed cathodes in a continuously running arc system. Ultrahigh purity (99.99% pure) argon was used as plasma forming gas. An external magnetic field of 0.10 T was used to rotate the arc, which was operated at a constant power of 6 kW (40 V). Cathodes having microstructures with mean grain sizes, ranging from 1.12 to 3.06 μm, were produced using cold spraying (CS) and annealing methods. CS cathodes were tested in their as-sprayed state and annealed state. Annealed CS coatings with near equi-axed grains of 2.29 μm average size gave 60% higher steady-state arc velocities and up to 50% lower erosion rates than massive copper cathodes having 20-23 μm average grain size. An effect of cathode microstructure on arc velocity and on arc erosion rates was observed.

Keywords cold gas dynamic spraying, erosion and abrasion resistance, heat treatment of coatings

1. Introduction

Thermal plasma technology plays an important role in materials processing and waste treatment (Ref 1). Plasma torches using cold cathodes in tubular geometry are used for high-power applications such as melting, cutting, and spraying (Ref 2). Erosion of electrodes limits the application of these torches into many industries. The erosion of electrodes results in their short lifetimes and frequent replacement, thereby increasing the operating cost of a plasma system. Previous studies on cold cathode plasma torches have shown that the degree of erosion of the cathode is far greater than that of the anode (Ref 1, 3). Thus, much importance has been placed on finding methods to reduce cathode erosion.

Cathode erosion is a complex process affected by many operating parameters such as the magnetic field strength used to rotate the arc, plasma gas chemistry, arc current and voltage, as well as the characteristics of the electrodes such as the electrode chemistry, geometry, and the cathode microstructure (Ref 3-6). Researchers have shown an effect of cathode microstructure on arc attachment, movement, and on its erosion rates (Ref 7). Wang and co-workers, working with nanostructured CuCr alloy cathodes and $Cu_{60}Zr_{28}Ti_{12}$ cathodes, observed that the erosion rates on these electrodes were lower compared to conventional cathodes (4-20% less than massive Cu) (Ref 7).

An earlier study in our group has shown that, for vacuum arcs, nano-structured cathodes produced by atmospheric pressure plasma spraying (PS) and high-velocity oxy fuel (HVOF) spraying give lower erosion rates than massive copper cathodes with relatively large grain sizes (Ref 6). In addition to their nano-structured grains, electrodes produced by PS and HVOF methods have intersplat oxygen content of ~2 at.%. It is known that the presence of oxygen in the cathode reduces its erosion rate (Ref 8). Hence, the low degree of erosion reported by Rao et al. may be due to the nano-structure of the coatings and/or the oxide content of the coated cathode (Ref 6). Isolating the effect of microstructure from the oxide content and studying its effect on arc erosion is of fundamental interest. Cold spraying (CS) can produce oxide-free coatings having grain sizes in the microscale rather than nano-metric range (Ref 9). Hence, cold-sprayed cathodes are ideal for isolating the effect of microstructure only on erosion behavior.

Rao has shown that cathodes with small grain sizes have higher arc velocities and hence low erosion rates (Ref 6, 10). Therefore, cold-sprayed coatings having smaller grain sizes than massive copper cathodes are expected to have higher arc velocities and, possibly, lower erosion rates than massive copper. However, due to weak intersplat bonding and substrate-coating bonding, CS as-sprayed coatings have lower electrical and thermal conductivities than pure copper (Ref 11). As erosion of cathodes is primarily controlled by heat removal from the cathode, having a low thermal conductivity coating may

Keith D'Sa, Lakshminarayana Rao, and **Richard J. Munz**, Department of Chemical Engineering, McGill University, Montreal, QC, Canada H3A 2B2. Contact e-mail: narayana.rao@gmail.com.

not reduce erosion. However, heat treatment of CS coatings is known to improve the electrical and thermal transport properties as well as the metallic bonding of the coating (Ref 11). Li et al. have shown that, for CS copper coatings sprayed on Cu substrates, annealing enhances adhesion of the coating to its substrate as well as metallic bonding between the splats (Ref 11).

In this article, we report on the effect of microstructure on the arc erosion behavior of copper cathodes. CS copper coatings having submicron to a few micron grain sizes in their as-sprayed and annealed state were tested for arc erosion behavior. The results obtained were compared with massive copper (M-Cu), having 20-23 μm grain size. Erosion behavior was characterized by the erosion rates, arc rotation velocities, and morphology of eroded cathodes.

2. Materials and Experimental Methods

2.1 Characterization of Powders

Amperit 190 (gas-atomized, 99.99% pure copper powder, oxygen content 500 ppm max; further referred to as A-190) was used as the spray powder for cold spraying. The morphology of the powder was studied using field emission scanning electron microscopy (SEM), whereas the particle size distribution was determined using the Mastersizer-2000 particle size analyzer (PSA) with distilled water as the dispersant. Energy dispersive spectroscopy (EDS) and inductively coupled plasma mass spectroscopy (ICP) were used to determine the chemical composition of A-190.

2.2 Preparation of Cathodes

Two different substrates, square copper plates (60 × 60 × 2.5 mm) and oxygen-free, high conductivity, 99.99% pure copper hollow cylinders (25 mm outer diameter, 65 mm length), were used for CS spraying. All the substrates were grit blasted with 708 μm alumina grits just before coating and had a surface roughness Ra of 8.58 μm. The spraying process was carried out with the Kinetics 3000 cold-spray gun (Cold Gas Technology Gmbh), at a chamber pressure of 32 bar and 500 °C. Summary of the spray condition is given in Table 1

The CS-coated hollow cylinders and copper plates were annealed in an argon atmosphere in a tubular furnace. A full factorial two temperature (300 and 600 °C), two annealing times (1 and 8 h) experimental design was chosen for annealing. Before starting the annealing procedure, the specimens were placed inside the tubular furnace and the furnace was flushed with ~90 furnace volumes of 99.99% pure argon gas flowing at 3 slpm. After purging, the heating was started, maintaining the argon flow rate to reach the desired annealing temperature. It took less than 10 min to reach the desired annealing

Table 1 Cold spray parameters

Pressure, bar	32
Spray distance, mm	40
Rotation speed, rpm	272
Propellant gas	Nitrogen
Propellant gas flow rate, m^3/h	3
As-sprayed coating thickness, μm	350 ± 25

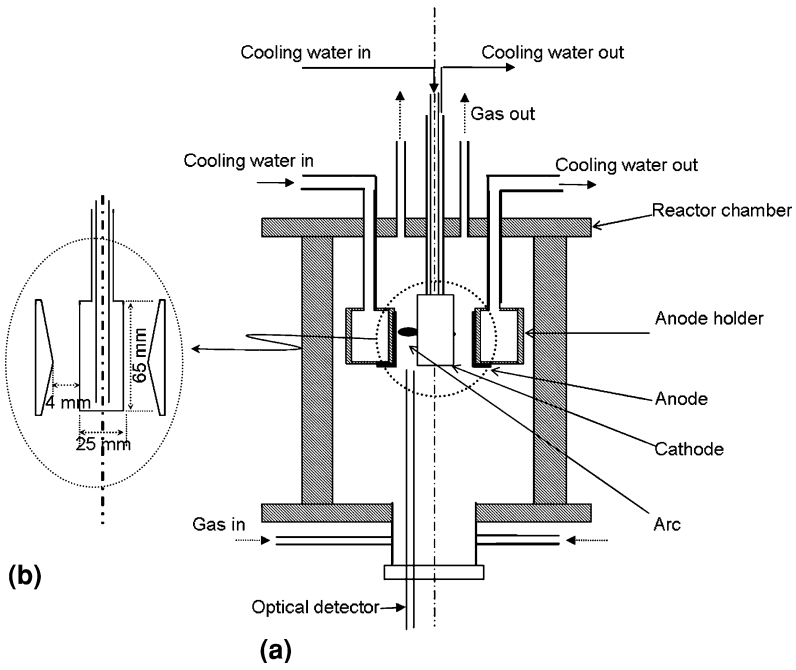

Fig. 1 Schematic diagrams of (a) the continuous-arc reactor and (b) the electrode setup

temperature. The specimens were held at this temperature for either 1 or 8 h. Then the heating was stopped and the specimens were allowed to cool to room temperature inside the furnace, while still maintaining the argon flow. Annealed cylinders were used as cathodes for erosion studies whereas Cu plates were used for microscopic analysis.

For microscopic analysis, the coatings on Cu plates were cut using a Struers 'Secotom-10' universal precision cut off machine and vacuum mounted in cold setting resin. The mounted specimens were wet ground using SiC paper #800, 1200, and 4000 under running tap water. The ground samples were the polished using 3 and 0.04 μm silica suspensions. The polished samples were etched with a $FeCl_3$ etchant (2.5 g $FeCl_3$ + 10 mL HCl + 50 mL ethanol) for 5 s. The etched coatings were examined under optical microscope and SEM to determine their microstructure. To determine the porosity of the coatings, as many as 10 SEM pictures of polished coatings (prior to etching) were taken at regular intervals on each of the coatings and the porosity of individual pictures was measured by an image analysis technique. An average of these numbers were calculated and reported as porosity with a standard deviation of ±5% of the average. SEM pictures of etched coatings were used to calculate grain sizes. An average and standard deviation of the grain size measurements taken from multiple SEM pictures of a given coating was calculated and are reported here.

2.3 Erosion Setup and Procedure

Figure 1 is a schematic diagram of the erosion apparatus. Figure 1(a) shows an overview of the setup while Fig. 1(b) gives the electrode dimensions. It was only practical to coat hollow cylinders externally, so the water-cooled coated hollow cylinder was used as cathode, surrounded by a sleeve anode, with a minimum annular gap of 4 mm. Both electrodes were water-cooled. A water-cooled solenoid around the electrode assembly was used to apply an axial magnetic field of 0.10 T to rotate the arc. The axial magnetic field strength varied less than 3% radially and 5% axially within the test cathode. The arc was ignited by a high-frequency trigger pulse and powered by a welding power supply (maximum power and current of 78 kW and 500 A, respectively). An average power of 6 kW (40 V and 150 A) was maintained throughout the experiment. Experiments were conducted using ultrahigh purity (99.99% pure) argon as the plasma forming gas, which circulated from the lower end of the reactor to the top end at a flow rate of 23 slpm under atmospheric pressure.

The cathode was weighed to an accuracy of $\pm 5 \times 10^{-4}$ g and installed in the reactor. An optical detector as shown in Fig. 1(a) was used to capture the arc rotation frequency. It consisted of a photodiode and a collimating lens assembly having a narrow field of view of 3 mm. The optical detector assembly was aligned to view the arc

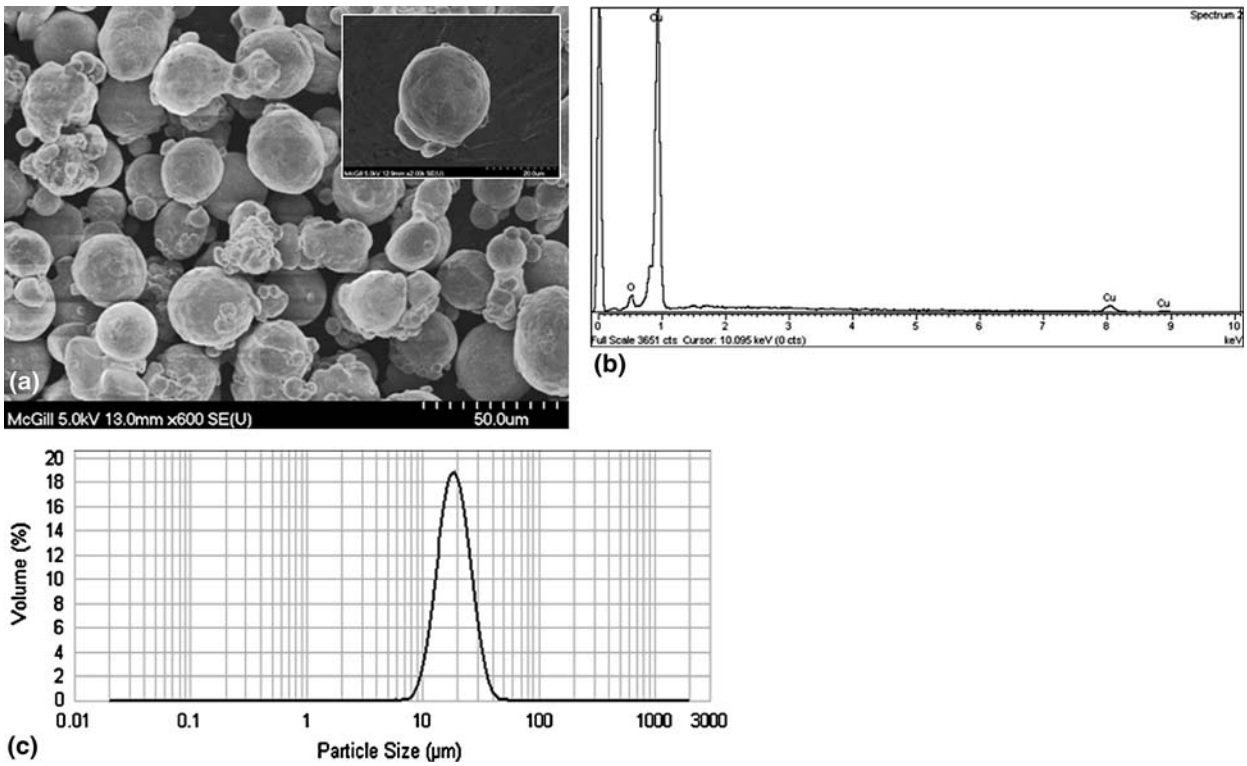

Fig. 2 Characterization of A-190 particles: (a) Morphology and an individual particle (inset), (b) energy dispersive spectrum, and (c) particle size distribution

between the electrodes and gave a positive voltage output when the arc passed its field of view. This optical voltage output, the arc current, and arc voltage waveforms were recorded simultaneously onto a computer using LabVIEW at 10 kHz sampling rate. After the erosion experiment, the cathode was removed from the reactor and dried of cooling water completely before recording its final weight. The erosion rate values in grams per coulomb were calculated by dividing the weight difference of the cathode before and after arcing by the total electric charge, $Q = \int I\,dt$, passing through the cathode. The arc rotation frequency was calculated from the recorded optical voltage data using windowed fast Fourier transform analysis. For each type of cathode, two individual experiments were performed and an average erosion rate and standard deviation were determined and reported.

3. Results and Discussion

3.1 Characterization of Powders

Figure 2(a) shows an SEM image of A-190. In Fig. 2(a), the main picture shows the morphology of the powder and the inset shows an individual particle. We see that, most particles were spheroids and only a few appeared as agglomerates. The energy dispersive spectrum, shown in Fig. 2(b), revealed only peaks for Cu and O. The oxygen peak was attributed to surface oxidation of copper. The particle size distribution, shown in Fig. 2(c), was log normal ranging between 7 and 50 μm, with a peak at 20 μm. ICP analysis of the powder revealed it to be 99.99% pure copper, with no detectable contaminants.

3.2 Characterization of As-Sprayed Coatings

3.2.1 Porosity and Grain Size. Figure 3(a) shows an SEM image of an unetched cross-section of CS as-sprayed coatings. We see that the CS-as-sprayed coating was dense and had a coating porosity of $<1\%$. After etching, the intersplat boundaries and the grain boundaries were visible as shown in Fig. 3(b). Grain size measurement of CS-as-sprayed coatings showed that the average grains of CS-as-sprayed coatings were 1.17 ± 0.26 μm. Average grain sizes of CS-as-sprayed coatings are shown in Fig. 4.

3.2.2 Oxygen Content. To check the O content in the coating, EDS spot analysis was performed on CS coatings, by holding the electron beam at a single spot on the intersplat boundary. The result obtained was compared with a similar analysis on HVOF coatings and is shown in Fig. 5. We see that, both CS and HVOF coatings had carbon, copper, and oxygen peaks. The carbon peak was attributed to carbon contamination within the microscope and the O peak to the native oxide layer present on the Cu powder used to make the coatings. A closer look at the oxygen peak, shown in the inset of Fig. 5, reveals that, CS coatings had a small oxygen peak compared to HVOF coatings, which had ~2 at.% of O. This small O peak was in agreement with the O content quoted by the manufacturer, which was 500 ppm max. Low oxide content is typical of CS coatings since the CS coatings were formed without melting the copper particles.

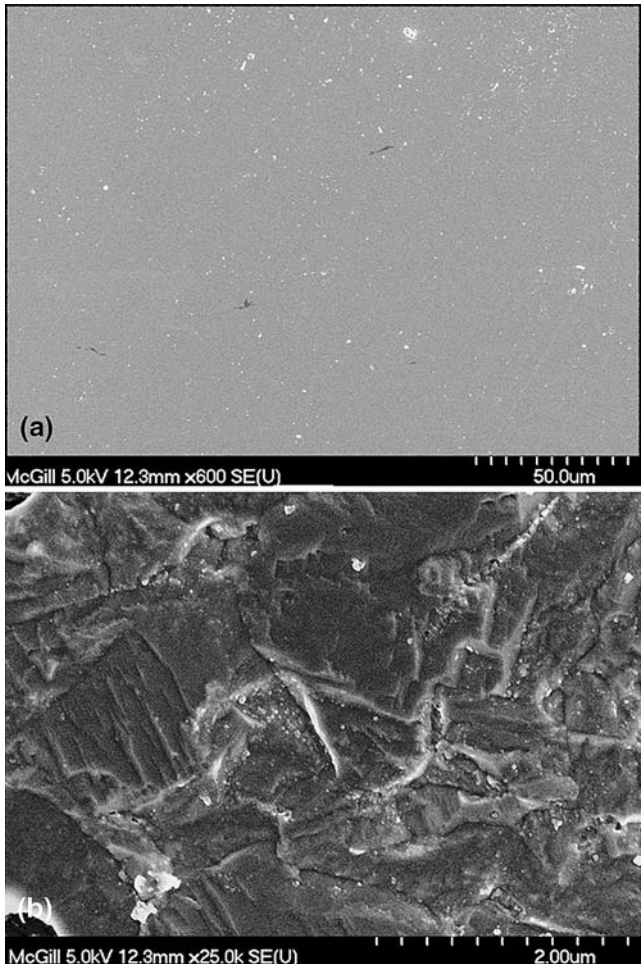

Fig. 3 (a) Unetched cross-section and (b) etched cross-section of as-sprayed coatings

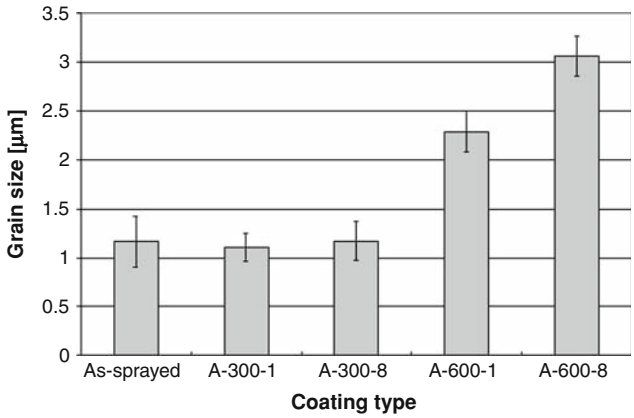

Fig. 4 Average grain size measurements for as-sprayed and annealed coatings

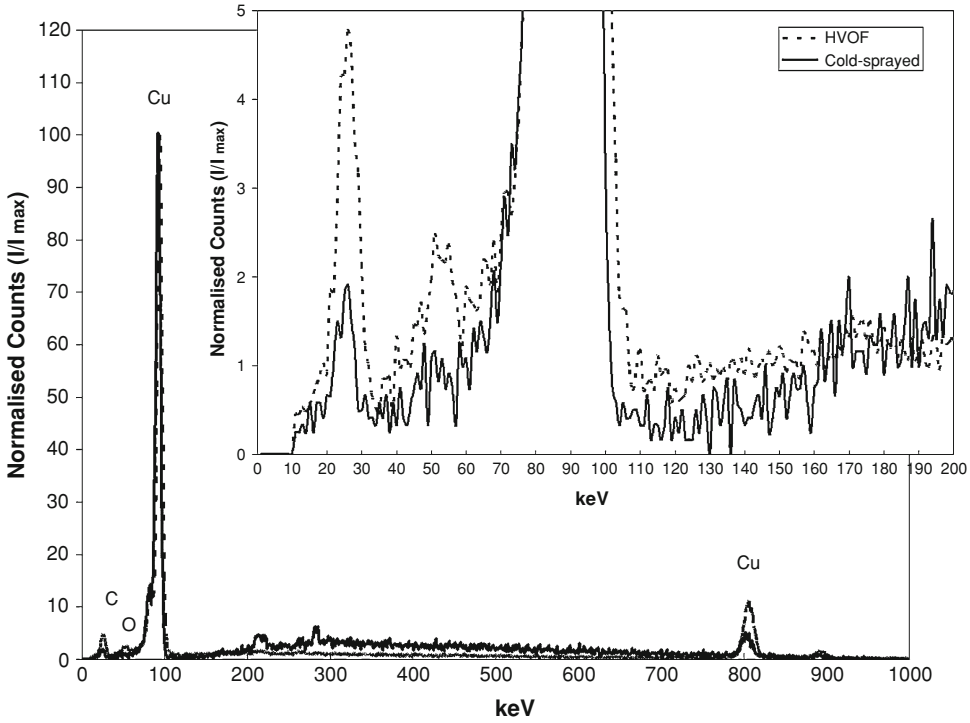

Fig. 5 EDS spot analyses of HVOF and CS coatings showing carbon, oxygen, and copper peaks. Notice the higher oxygen peak for HVOF coatings than CS coatings (inset)

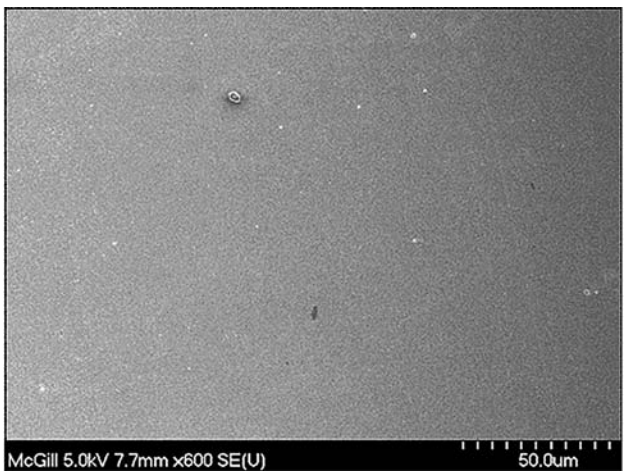

Fig. 6 Unetched cross-section of an A-300-1 coating

3.3 Characterization of Annealed Coatings

Figure 6 shows an SEM image of an unetched CS coating annealed at 300 °C for 1 h (referred to as A-300-1). Similar images were taken of CS coatings annealed at 300 °C for 8 h (referred as A-300-8) and CS coatings annealed at 600 °C for 1 and 8 h (referred as A-600-1 and A-600-8, respectively). All images show a dense coating with porosities of $<1\%$. Based on these results, it was concluded that heat treatment did not increase the porosity of cold-sprayed coatings.

Figure 7(a) to (d) are SEM images of etched A-300-1, A-300-8, A-600-1, and A-600-8 coatings, respectively. Average grain-size measurements taken from similar images are reported in Fig. 4. We can see a clear effect of annealing at high temperatures on the microstructure of these coatings. Figure 4 and 7 shows that annealing at 300 °C does not promote grain growth through diffusion. Hence, the grain sizes reported for as-sprayed, A-300-1, and A-300-8 coatings are similar (1.17 ± 0.26, 1.11 ± 0.14, and 1.17 ± 0.20 μm, respectively). Annealing at 600 °C, however, induces significant grain growth. We also see that the coatings annealed for 8 h had grains which were 33% larger than those annealed for 1 h only. The average grain sizes for A-600-1 and A-600-8 coatings were 2.29 ± 0.21 and 3.06 ± 0.21 μm, respectively. As shown in Fig. 7, the grains formed on all the coatings were equi-axed. Figure 4 summarizes the average grain measurement of all the coatings. Among all the coatings formed, A-600-8 coatings had the largest grains measuring 3.06 ± 0.21 μm. Our observations are similar to the findings of Li et al. (Ref 11).

3.4 Arc Velocity and Erosion Results

3.4.1 Arc Velocity and Erosion Results for Central M-Cu Cathodes. Since the central cathode geometry was used for cold-sprayed cathodes, it was necessary to obtain erosion results for M-Cu in a similar setup. These results could be used as a base line to compare with the arc velocity and erosion rates of CS coatings. The full details of the erosion measurement on central M-Cu are

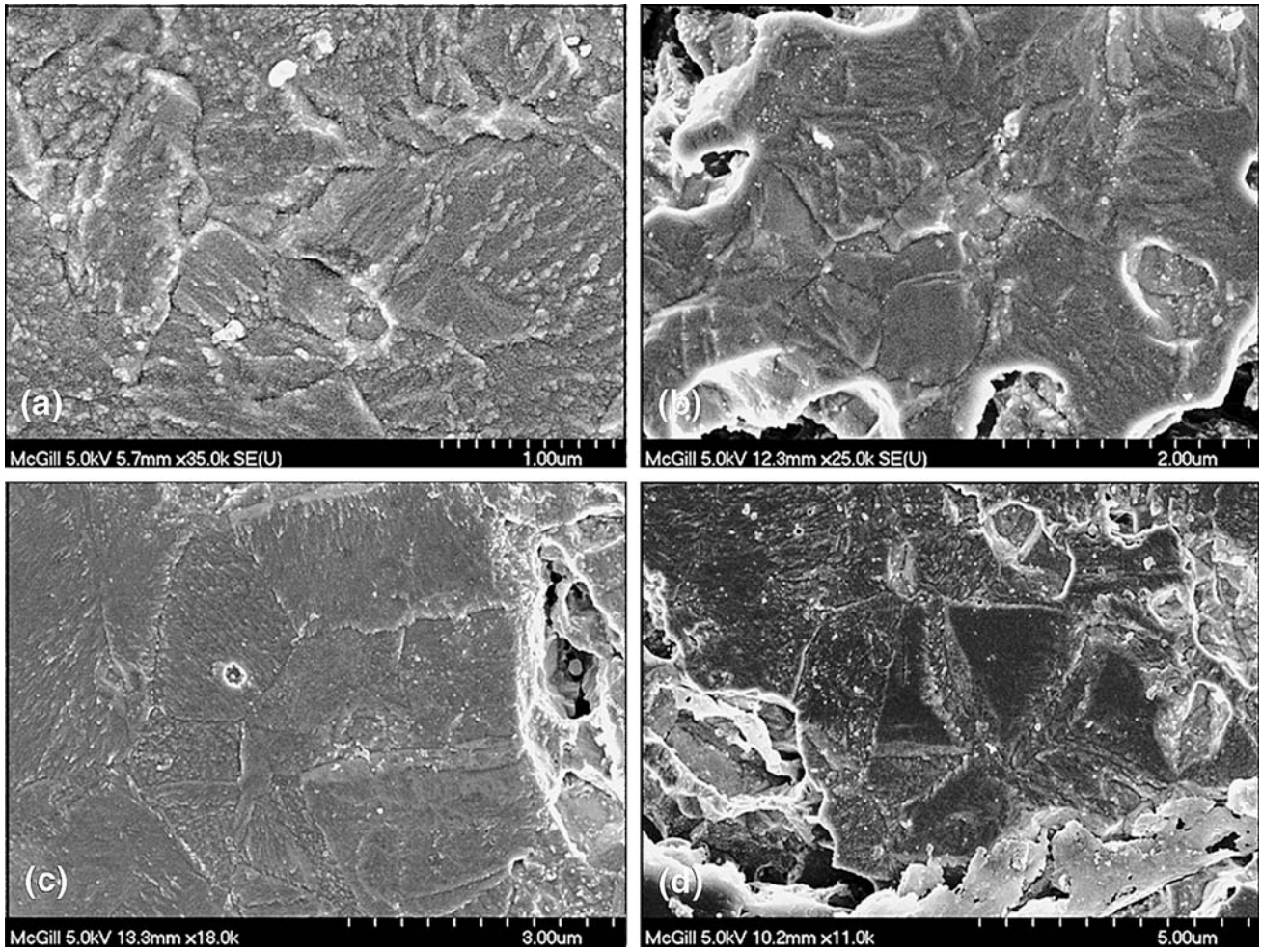

Fig. 7 Images of grain structures taken from etched cross-sections of (a) A-300-1, (b) A-300-8, (c) A-600-1, and (d) A-600-8 coatings

presented elsewhere (Ref 1, 3, 8, 12, 13). The erosion rate of M-Cu cathodes in argon atmosphere for an arc time of 6 min is 47 ± 5 μg/C.

3.4.2 Arc Velocity and Erosion Results of As-Sprayed and Annealed CS Cathodes. Figure 8 shows typical arc velocities of as-sprayed cathodes after 4 min of arcing. Arcing was stopped after 4 min due to spalling of the coating. We see from Fig. 8 that, unlike M-Cu, the arc velocity on as-sprayed coatings has only one unsteady regime where it oscillates between 45 and 10 m/s. For M-Cu, the arc rotation velocity starts off at 55 m/s but eventually drops below 6.6 ± 0.6 m/s after 200 s of arcing. Figure 9 shows an eroded, as-sprayed cathode. Severe spalling of the coating is evident from Fig. 9. This spalling, which is catastrophic in nature, is believed to be the reason for the unsteady velocities seen on as-sprayed coatings. Although the mean arc velocities on as-sprayed coatings were higher than that of M-Cu, we cannot draw any conclusion on the effect of microstructure on arc velocity and erosion rates due to severe spalling of the coating. The erosion rates for as-sprayed coatings, after 4 min of arcing, are shown in Fig. 10. Severe spalling was the reason for higher erosion values on these CS-as-sprayed cathodes. Hence, further efforts were made to reduce spalling of the coatings by annealing.

To test the effect of annealing, CS coatings were annealed at 300 and 600 °C for 1 and 8 h duration, respectively. Annealing at 600 °C for 8 h caused swelling of the coating and blister formation on the cathodes, as shown in Fig. 11. We believe that gases trapped in the pores of the coating caused blistering upon annealing. Blistering was only observed for A-600-8 case.

Figure 12 shows the annealed cathodes after 4 min of arcing. As can be seen from Fig. 12, all coatings except A-600-1 coatings spalled. Figure 10 shows the erosion rates of annealed cathodes. Again, high erosion rates were due to severe spalling of the coatings. The results suggest that annealing at 300 °C for both 1 and 8 h do not reduce spalling. Annealing at 600 °C for 8 h causes blistering of the coating, thereby increasing the contact resistance between the coating and substrate. This leads to higher erosion rates. However, cathodes annealed at 600 °C for 1 h show low spalling. Hence these coatings were arced for a length of 6 min.

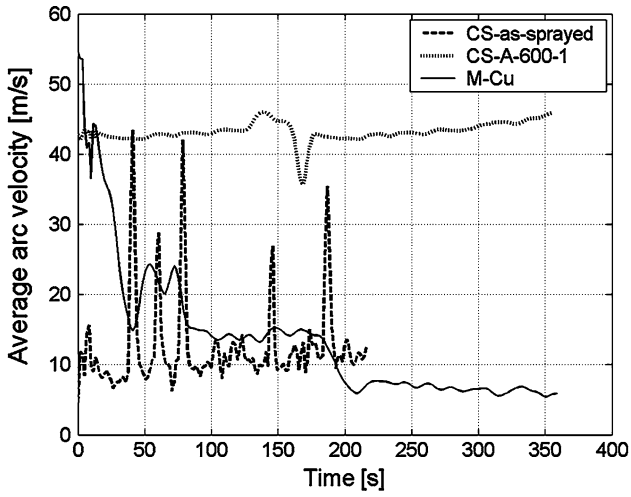

Fig. 8 Arc velocity as a function of time for as-sprayed, A-600-1, and massive Cu

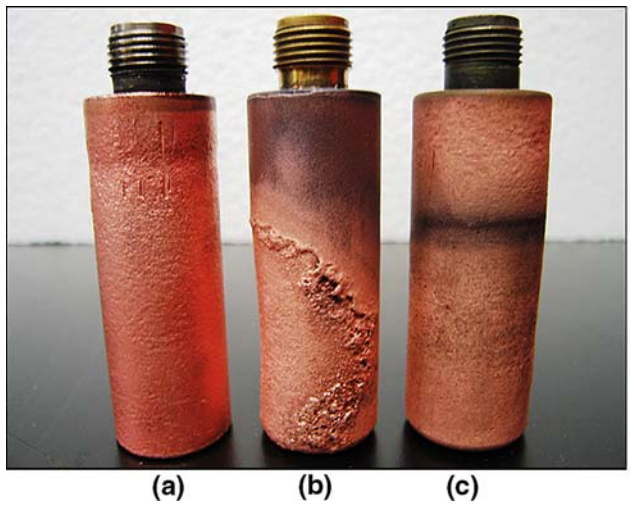

Fig. 9 (a) M-Cu, (b) as-sprayed, and (c) A-600-1 cathodes after erosion. Notice the severe spalling of the as-sprayed cathode. Both M-Cu and A-600-1 cathodes remained intact after erosion

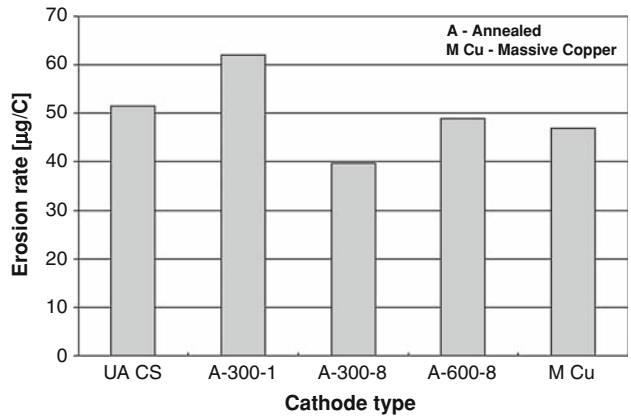

Fig. 10 Average erosion rates for coated and M-Cu cathodes

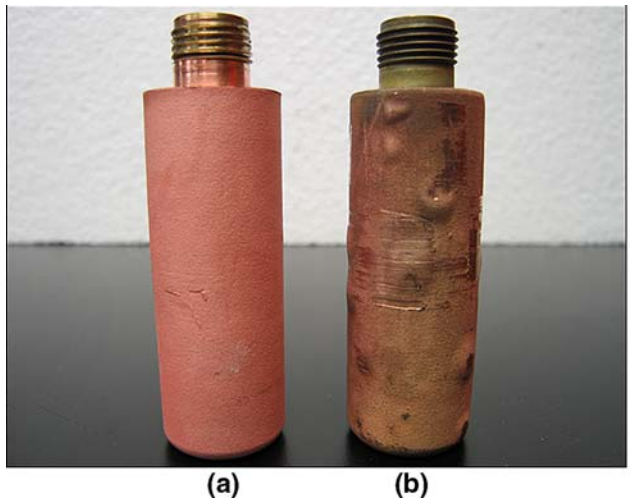

Fig. 11 (a) As-sprayed and (b) A-600-8 cathodes before erosion. Notice the swelling of the coating after annealing at 600 °C for 8 h

Figure 8 shows typical arc velocity results for A-600-1 coatings. The arc velocity for A-600-1 cathodes had one fast steady regime (arc velocity of ~43 m/s), unlike M-Cu. A-600-1 cathodes (average grain size of 2.29 µm) differed from M-Cu cathodes (average grain size of 21.5 µm) only in their grain sizes. Hence, the high arc velocity was attributed to the difference in the microstructure of the cathode. These results show a clear effect of microstructure on arc velocity. As a result of a high arc velocity, A-600-1 cathodes had lower erosion rates than M-Cu. These erosion results are presented in Fig. 13. For an arc time of 6 min, the average erosion rate for A-600-1 cathodes was 21.92 ± 5.38 µg/C, which is 35% lower than that of M-Cu.

From Fig. 4 and 8, it is clear that even though A-600-1 cathodes had larger grain sizes than as-sprayed cathodes, they had higher arc velocities. This contradicts the argument that small grain sizes result in high arc velocities. However, on paying close attention to Fig. 8, one can observe large fluctuations in the arc velocity for as-sprayed cathodes, from 10 m/s to levels reported for A-600-1 cathodes. This leads us to believe that as-sprayed cathodes do have high arc rotation velocities, which cannot be reached due to spalling of the coating (shown in Fig. 12). The heat treatment applied to A-600-1 cathodes improved intersplat and coating-substrate adhesion and hence prevented spalling and maintained high arc velocities.

3.5 Characterization of Eroded Cathodes

SEM analysis of cold-sprayed cathodes showed no changes in grain sizes in the bulk of the coatings. Hence, the same grain sizes as those given in Fig. 4 were measured for

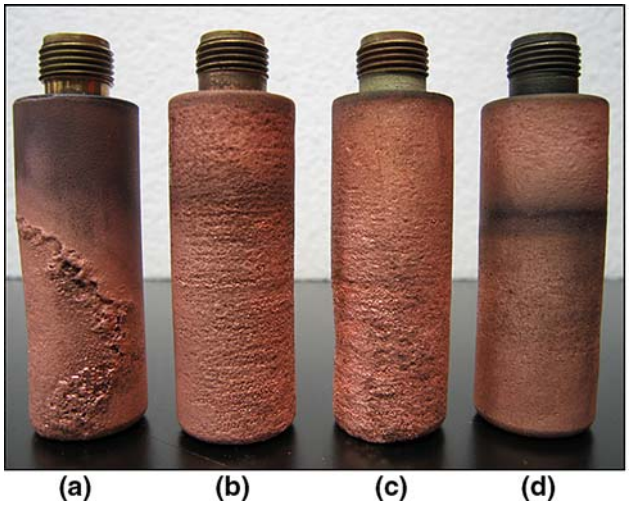

Fig. 12 (a) As-sprayed, (b) A-300-1, (c) A-300-8, and (d) A-600-1 cathodes after 4 min of arcing. Notice the spalling on all cathodes except A-600-1

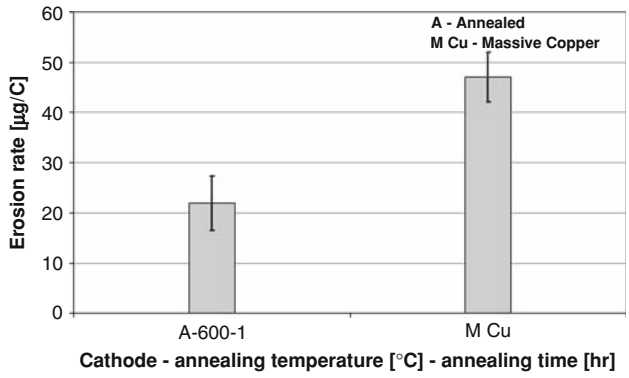

Fig. 13 Average erosion rates for M-Cu and A-600-1 cathodes

eroded cathodes as well. However, only a thin layer in the outmost splats, which came in direct contact with the arc showed smaller grains, indicating melting and rapid solidification. Figure 14 shows an outmost splat of an eroded A-600-1 coating. This region contains smaller grains than bulk of the coating. Since the bulk of the coating was unaffected by arcing, it was concluded that the initial microstructure was preserved even after erosion experiments.

4. Conclusions

Cold-sprayed cathodes were tested in a continuous arc chamber to study the effect of microstructure on erosion. The analysis of the coatings formed show that CS cathodes had insignificant oxide content and hence, could be used to isolate the effect of microstructure on erosion. Arc velocities on CS-as-sprayed coatings were fluctuating and spalling is believed to be the reason for such fluctuations

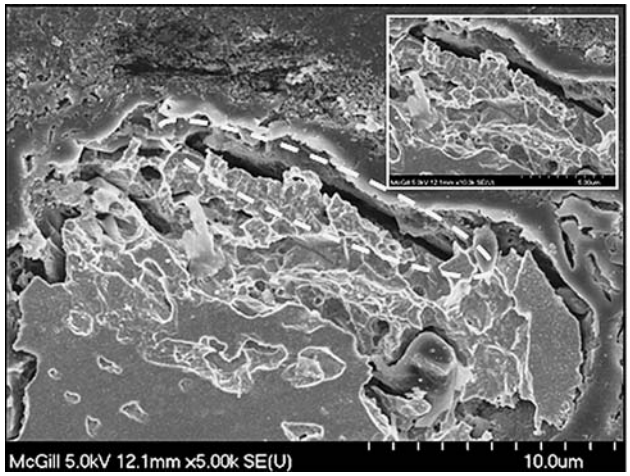

Fig. 14 Etched cross-section of an eroded, as-sprayed coating. The highlighted area shows an arced region

in arc velocity. CS cathodes annealed at 600 °C for 1 h gave low erosion rates due to their improved transport properties and metallic bonding. These cathodes which had smaller grains than M-Cu gave higher arc velocities and lower erosion rates.

The results show a clear effect of cathode microstructure on erosion behavior of cold cathodes. We conclude that the microstructure of the cathode affects the arc rotation velocity in a magnetically driven atmospheric pressure arc system. Having grain size distribution in the submicron and/or nanometric range results in higher arc velocities and hence lower erosion rates.

Acknowledgments

The authors would like to thank Dr. Christian Moreau and Dr. Jean-Gabriel Legoux of IMI, Montreal, Canada for producing the coatings and providing valuable knowledge on the subject matter, and the EUL funds for their financial support.

References

1. R.N. Szente, R.J. Munz, and M.G. Drouet, Electrode Erosion in Plasma Torches, *Plasma Chem. Plasma Process.*, 1992, **12**(3), p 327-343 (in English)
2. P. Fauchais and A. Vardelle, Thermal Plasmas, *IEEE Trans. Plasma Sci.*, 1997, **25**(6), p 1258-1280 (in English)
3. R.N. Szente, R.J. Munz, and M.G. Drouet, The Effect of Low Concentrations of a Diatomic Gas in Argon on Erosion on Copper Cathodes in a Magnetically Rotated Arc, *Plasma Chem. Plasma Process.*, 1987, **7**(3), p 349-364 (in English)
4. P. Tsantrizos and W.H. Gauvin, Cathode Erosion Phenomena in a Transferred-Arc Plasma Reactor, *Plasma Chem. Plasma Process.*, 1992, **12**(1), p 17-33 (in English)
5. J.E. Harry, The Measurement of the Erosion Rate at the Electrodes of an Arc Rotated by a Transverse Magnetic Field, *J. Appl. Phys.*, 1969, **40**(1), p 265-270 (in English)
6. L. Rao, R.J. Munz, and J. Meunier, Vacuum Arc Velocity and Erosion Rate Measurements, *J. Phys. D: Appl. Phys.*, 2007, **40**(14), p 4192-4201 (in English)

7. C. Zhang, Z. Yang, Y. Wang, and B. Ding, Cathode Spot Propagation on the Surface of Amorphous, Nanocrystalline, Crystalline $Cu_{60}Zr_{28}Ti_{12}$ Cathodes, *Phys. Lett. A*, 2003, **318**(4), p 435-439 (in English)
8. R.N. Szente, R.J. Munz, and M.G. Drouet, Cathode Erosion in Inert Gases: The Importance of Electrode Contamination, *Plasma Chem. Plasma Process.*, 1989, **9**(1), p 121-132 (in English)
9. F. Gartner, T. Stoltenhoff, J. Voyer, H. Kreye, S. Riekehr, and M. Koçak, Mechanical Properties of Cold-Sprayed and Thermally Sprayed Copper Coatings, *Surf. Coat. Technol.*, 2006, **200**(24), p 6770-6782 (in English)
10. L. Rao, ''Chapter 6: Effect of Cathode Microstructure on Erosion of Copper Cathodes—An Experimental Study,'' McGill University, Montreal, Quebec, Canada, 2007
11. W. Li, C. Li, and H. Liao, Effect of Annealing Treatment on the Microstructure and Properties of Cold-Sprayed Cu Coating, *J. Therm. Spray Technol.*, 2006, **15**(2), p 206-211 (in English)
12. L. Rao, ''Chapter 7: Effect of Cathode Microstructure on Erosion of Copper Cathodes—An Experimental Study,'' McGill University, Montreal, Canada, 2007
13. R.N. Szente, ''Erosion of Plasma Torch Electrodes,'' Ph.D. Thesis, McGill University, Montreal, Canada, 1989